Astronomy and Space Science: Open Access
Received: Jun 13, 2016, Accepted: Aug 01, 2016, Published: Aug 05, 2016
Astron Space Sci, Volume 2, Issue 1
http://crescopublications.org/pdf/assoa/ASSOA-2-009.pdf
Article Number: ASSOA-2-009

Research Article Open Access

Study of Whistler Mode Waves for Loss Cone Distribution Function with Perpendicular AC Electric Field in Magnetosphere

R.S. Pandey[1], Rajbir Kaur[1], Shikha Bhadoria[1] and B.S. Tomar[2]

[1]Department of Applied Physics, Amity Institute of Applied Sciences, Amity University, Noida, U.P, India
[2]Department of Applied Physics, Magadh University, Bodh Gaya, India

***Corresponding Author:** Rajbir Kaur, Department of Applied Physics, Amity Institute of Applied Sciences, Amity University, Noida, U.P, India, E-mail: rkaur2@amity.edu; rspandey@amity.edu

Citation: R.S. Pandey, Rajbir Kaur, Shikha Bhadoria and B.S. Tomar (2016) Study of Whistler Mode Waves for Loss Cone Distribution Function with Perpendicular AC Electric Field in Magnetosphere. Astron Space Sci 2: 009.

Abstract

Whistler mode instability having field lines propagation for pitch angle loss cone unperturbed distribution function has been done for magnetoplasma in the presence of AC electric field perpendicular to the ambient magnetic field. The dispersion relation and growth rate have been derived and calculations are performed for magnetoplasma. The present analysis shows that the growth rate of electromagnetic circularly polarized whistler mode wave has been found to be increasing with temperature anisotropy and loss cone angle. It is also inferred that even in the absence of temperature anisotropy, there is growth of whistler waves, implying dominant role played by loss-cone angle in generating whistler mode instability. Also frequency of AC electric field modifies the resonant frequency conditions of Doppler shift.

Keywords: Whistler mode instability; Loss cone distribution function.

1. Introduction

The immediate environment of Earth consists of (i) the neutral atmosphere, extending up to 60 km above the Earth's surface, (ii) the ionosphere, a region of highly ionized gas (heavy ions, protons and electrons) as well as neutral particles extending up to 1000 km altitude and (iii) the magnetosphere, consisting mainly of protons and electrons extending up to a distance of ~ 100,000 km from Earth. The structural and physical processes of a magnetosphere are controlled mainly by the Earth's magnetic field and the energy from the sun. This energy arrives at the Earth in different forms and is deposited at different locations. Some of this energy is introduced at the outer boundary by the solar wind. The solar wind is a stream of charged particles ejected from the upper atmosphere of the Sun. It mostly consists of electrons and protons with energies usually between 1.5 and 10 keV. The solar wind is prevented from reaching the Earth itself by the effect of Earth's magnetic field. A good approximation to the Earth's magnetic field in this region is that of a centered dipole inclined with respect to the rotation axis by about 11°. The Earth has a magnetic field with north and south poles. The Earth's magnetic field reaches 36,000 miles into space. A magnetosphere is formed when a stream of charged particles, such as the solar wind, interacts with and is deflected by the magnetic field of a planet or similar body.

The magnetosphere prevents most of the particles from the sun, carried in solar wind, from hitting the Earth. Some particles from the solar wind can enter the magnetosphere. The particles that enter from the magneto tail travel toward the Earth and create the auroral oval light shows. There exist different sources of free energy in magnetosphere that give rise to instabilities. For example uneven distribution of temperature, energy density, magnetic field etc. Electromagnetic modes of waves generally become unstable due to presence of anisotropy of velocity distribution function of particles.

Coherent whistler emissions can result from phase bunching of energetic electrons triggered by external emissions or by incoherent whistler waves [1]. The scattering electrons into the loss cone by incoherent whistler radiation was considered by Kennel and Petschek [2], while pitch angle scattering caused by coherent whistler emissions was treated by Inan et al. [3]. The growth rate and frequency generated were evaluated at equatorial height and for low latitude region magnetosphere. The studies indicate the effects of pitch angle anisotropy and temperature anisotropy for hot energetic electrons on growth rate and emission frequencies. Huang et al. [4] calculated the characteristics of the incoherent whistler mode waves generated in the magnetosphere along the L = 5 geomagnetic field line which intersect the atmosphere in the region where the pulsating aurora is frequently observed and considered their implications for the pulsating aurora. They observed for the loss-cone driven Whistler instability, the growth rate along the L = 5 field line in largest just above the ionosphere where the loss-cone angle is also large.

In recent past, interest has been generated in studying and analyzing various distribution functions. Xiao et al. [5] provided the growth rate of field-aligned whistler mode waves in space plasma by using newly developed kappa-loss-cone (KLC) distribution, undergoing a fully relativistic treatment. Numerical calculations carried out for a direct comparison between the new KLC distribution and the current kappa distribution, revealed that in the lower wave frequency, the wave growth by KLC distribution is higher than that by the kappa distribution because of larger fractional number of the resonant electrons (which controls the wave growth) for KLC distribution, but it is lower in higher wave frequency. It indicated an important role played by hot electrons with typical energies of hundreds of keV in generating the instability of whistler mode waves. Prince and Renuka [6] presented the interaction of whistler waves with assumed anti-loss cone (ALC) distribution becoming highly unstable at times of substorm onset. It established the presence of ALC electrons at onset-time geomanetosphere plasma sheet. It was seen that whistler instability resulting from ALC interactions arises at frequencies greater the electron cyclotron frequency. The major part of free energy available at PS was proved to be the contribution due to anisotropy of ALC distribution function. Also presence of few cold electrons along with hot ALC plasma caused wave decay. Pandey et al. [7] reported whistler mode instability having propagation vector oblique to ambient magnetic field for pitch angle loss cone unperturbed distribution functions for inhomogeneous ionospheric plasma. Analytical studies suggested that growth rate of electromagnetic VLF waves was enhanced by free energy source like temperature anisotropy and loss-cone up to a limited angle of propagation.

Being inspired from above findings, in this paper whistler mode instability having field lines propagation for pitch angle loss cone unperturbed distribution function for magnetoplasma in the presence of perpendicular AC electric field to the ambient magnetic field is studied. The dispersion relation in growth rate have been derived and calculated for magnetoplasma. Parametric studies are performed by changing plasma parameters: temperature anisotropy, AC frequency, thermal velocity and loss-cone angle.

2. Dispersion Relation

A spatially homogeneous an isotropic, collision less magneto plasma subjected to an external magnetic field $\mathbf{B_o} = B_o\,\hat{e}_x$ and an electric field $\mathbf{E_0} = (E_0 \sin \upsilon t\,\hat{e}_x)$ has been considered in order to obtain the relation. In case, the Vlasov-Maxwell equations are lineralized. The linearlized equations obtained after neglecting the higher order terms and separating the equilibrium and non- equilibrium parts, following the techniques of Pandey et al. [8] are given as

$$\mathbf{v}\frac{\partial f_{s0}}{\partial r}.+\frac{e_s}{m_s}\left[\mathbf{E_o}\sin\upsilon t+(\mathbf{v}\times\mathbf{B_o})\right]\left(\frac{\partial f_{so}}{\partial v}\right)=0 \qquad \text{... (1)}$$

$$\frac{\partial f_{s1}}{\partial t}+\mathbf{v}.\frac{\partial f_{s1}}{\partial r}+\left(\frac{\mathbf{F}}{m_s}\right)\left(\frac{\partial f_{s1}}{\partial v}\right)=\mathbf{S}(r,v,t) \qquad \text{… (2)}$$

Where force is defined as $\mathbf{F} = m\,d\mathbf{v}/dt$

$$\mathbf{F} = e_s\,[E_0 \sin(\mathbf{v} \times \mathbf{B_0})] \qquad \text{... (3)}$$

The practical trajectories are obtained by solving the equation of motion defined in eq. (3) and **S**(r,v,t) is defined as:

$$\mathbf{x_0} = \mathbf{x} + \left(\frac{\mathbf{v_y}}{\omega_{cs}}\right) + \left(\frac{1}{\omega_{cs}}\right)\left[\mathbf{v_x}\sin\omega_{cs}t' - \mathbf{v_y}\cos\omega_{cs}t'\right] + \left(\frac{\Gamma_x}{\omega_{cs}}\right)\left[\frac{\omega_{cs}\sin\upsilon t' - \upsilon\sin\omega_{cs}t'}{\omega_{cs}^2 - \upsilon^2}\right]$$

$$\mathbf{y_0} = \mathbf{y} + \left(\frac{\mathbf{v_x}}{\omega_{cs}}\right) - \left(\frac{1}{\omega_{cs}}\right)\left[\mathbf{v_x}\cos\omega_{cs}t' - \mathbf{v_y}\sin\omega_{cs}t'\right] - \left(\frac{\Gamma_x}{\upsilon\omega_{cs}}\right)\left[1 + \frac{\upsilon^2\cos\omega_{cs}t' - \omega_{cs}^2\cos\upsilon t'}{\omega_{cs}^2 - \upsilon^2}\right]$$

$$\mathbf{z_0} = \mathbf{z} - \mathbf{v_z}t' \qquad \ldots (4)$$

and the velocities are

$$\mathbf{v_{x0}} = \mathbf{v_x}\cos\omega_{cs}t' - \mathbf{v_y}\sin\omega_{cs}t' + \left\{\frac{\upsilon\Gamma_x(\cos\upsilon t' - \cos\omega_{cs}t')}{\omega_{cs}^2 - \upsilon^2}\right\}$$

$$\mathbf{v_{y0}} = \mathbf{v_x}\sin\omega_{cs}t' + \mathbf{v_y}\cos\omega_{cs}t' - \left\{\frac{\Gamma_x(\omega_{cs}\sin\upsilon t' - \upsilon\sin\omega_{cs}t')}{\omega_{cs}^2 - \upsilon^2}\right\}$$

$$\mathbf{v_{z0}} = \mathbf{v_z} \qquad \ldots (5)$$

where $\omega_{cs} = \frac{e_s B_0}{m_s}$ is the cyclotron frequency of species s and $\Gamma_x = \frac{e_s E_0}{m_s}$ and AC electric field is varying as $E = E_{0x}\sin\upsilon t$, υ being the angular AC frequency.

$$\mathbf{S}(r,v,t) = \left(-\frac{e_s}{m_s}\right)\left[\mathbf{E_1} + \mathbf{v}\times\mathbf{B_1}\right]\left(\frac{\partial f_{so}}{\partial v}\right) \qquad \ldots (6)$$

where s denotes species and $\mathbf{E_1}$,$\mathbf{B_1}$ and $\mathbf{f_{s1}}$ are perturbed and are assumed to have harmonic dependence in $\mathbf{f_{s1}}$, $\mathbf{B_1}$ and $\mathbf{E_1}$ =~exp I(**k**, r-ωt).The method of characteristic solution is used to determine the perturbed distribution function.f_{s1}, which is obtained from eq. (2) by

$$\mathbf{f_{s1}}(r,v,t) = \int_{\circ 0^\circ}^{\infty} \mathbf{S}\{r_0(r,v,t`), \mathbf{v_0}(r,v,t`), t - t` dt` \qquad \ldots (7)$$

The phase space coordinate system has been transformed from (r,v,t) to (r_0,v_0,t-t`).The particle trajectories which have been obtained by solving eq.(3) for the given external field configuration and wave propagation $\mathbf{k} = \left[k_\perp \mathbf{e_x}, 0, k_\parallel \mathbf{e_z}\right]$.After doing some lengthy algebraic simplification and carrying out the integration, the perturbed distribution function f_1 is written as Pandey et al. [8].

$$\mathbf{f_{s1}}(r,v,t) = -\frac{e_s}{m_s\omega}\sum_{m,n,p,q}^{\infty}\frac{J_p(\lambda_2)J_m(\lambda_1)J_q(\lambda_3)e^{i(k.r-\omega t)}}{\{\omega - k_\parallel v_\parallel - (n+q)\omega_{cs} + p\upsilon\}}\left[\mathbf{E_{1x}}J_n J_p\left\{\left(\frac{n}{\lambda_1}\right)U^* + D_1\left(\frac{p}{\lambda_2}\right)\right\}\right.$$
$$\left. - i\mathbf{E_{1y}}\left\{J_n' J_p C_1 + J_n J_p' D_2\right\} + \mathbf{E_{1z}}J_n J_p W^*\right]$$

where the Bessel identity

$$e^{i\lambda\sin\theta} = \sum_{k=-\infty}^{\infty} J_k(\lambda)\, e^{ik\theta}$$

has been used, the arguments of the Bessel functions are

$$\lambda_1 = \frac{k_\perp v_\perp}{\omega_{cs}}, \lambda_2 = \frac{k_\perp \Gamma_x \upsilon}{\omega_{cs}^2 - \upsilon^2}, \lambda_3 = \frac{k_\perp \Gamma_x \omega_{cs}}{\omega_{cs}^2 - \upsilon^2}$$

where

$$C_1 = \frac{1}{v_\perp}\left(\frac{\partial f_0}{\partial v_\perp}\right)(\omega - k_\parallel .v_\parallel) + \left(\frac{\partial f_0}{\partial v_\parallel}\right)k_\parallel$$

$$U^* = C_1\left[v_\perp - \left\{\frac{\upsilon\Gamma_x}{\omega_{cs}^2 - \upsilon^2}\right\}\right]$$

$$W^* = \left[\left(\frac{n\omega_{cs}v_\parallel}{v_\perp}\right)\left(\frac{\partial f_0}{\partial v_\perp}\right) - n\omega_{cs}\left(\frac{\partial f_0}{\partial v_\parallel}\right)\right] + \left[1 + \left\{\frac{k_\perp \upsilon\Gamma_x}{\omega_{cs}^2 - \upsilon^2}\right\}\{(p/\lambda_2) - (n/\lambda_1)\}\right]$$

$$D_1 = C_1\left\{\frac{\upsilon\Gamma_x}{\omega_{cs}^2 - \upsilon^2}\right\}, D_2 = C_2\left\{\frac{\omega_{cs}\Gamma_x}{\omega_{cs}^2 - \upsilon^2}\right\}$$

$$J_n' = \frac{dJ_n(\lambda_1)}{d\lambda_1}, J_p' = \frac{dJ_p(\lambda_2)}{d\lambda_2} \qquad \ldots (8)$$

Following R.S Pandey et al. [8] the conductivity tensor $\|\sigma\|$ is written as

$$\|\sigma\| = -\sum \frac{e_s^2}{m_s\omega}\sum_{m,n,p,q}^{\infty}\int \frac{J_q(\lambda_3)S_{ij}d^3v}{\omega - k\upsilon - (n+q)\omega_{cs} + p\upsilon}$$

where

$$S_{ij} = \begin{Vmatrix} v_\perp \frac{n}{\lambda_1}(J_n)^2 J_p A & iv_\perp J_n B & v_\perp W^* \frac{n}{\lambda_1}J_n^2 J_p \\ v_\perp J_p A J_n J'n & v_\perp J_n' B & iv_\perp W^* J_p J_n J'n \\ v_\parallel J_n^2 J_p A & -iv_\parallel J_n B & v_\parallel W^* J_n^2 J_p \end{Vmatrix}$$

$$A = \left(\frac{n}{\lambda_1}\right)U^* + \left(\frac{p}{\lambda_2}\right)D_1, \qquad B = J_n' J_p C_1 + J_n' J_n D_2$$

From $J = \|\sigma\|.E_1$ and two Maxwell's curl equations for the perturbed quantities, we have

$$\left[\mathbf{k}^2 - \mathbf{k}.\mathbf{k} - \frac{\omega^2}{c^2}\varepsilon(k,\omega)\right].\mathbf{E_1} = 0$$

where

$\varepsilon(k,\omega) = 1 - \frac{4\pi}{i\omega}\|\sigma(k,\omega)\|$ is dielectric tensor

The Maxwellian distribution function with loss-cone angle θ_c taken from Huang et al. (1990) is written as

$$f_{so} = \frac{n_0}{M\pi^{3/2}\alpha_\perp^2\alpha_\parallel}\exp\left[-\left(\frac{v_\perp}{\alpha_\perp}\right)^2 - \left(\frac{v_\parallel}{\alpha_\parallel}\right)^2\right] \qquad \left|\frac{v_\perp}{v_\parallel}\right| > \tan\theta_c$$

where normalization constant M is given as

$$M = \frac{1}{\sqrt{\frac{1+\tan^2\theta_c}{A_T + 1}}}$$

$$\left\|\varepsilon_{ij}(k,\omega)\right\| = 1 + \sum \frac{4\pi\pi_s^2}{m_s\omega^2}\int \frac{J_q(\lambda_3)\left\|S_{ij}\right\| d^3v}{\omega - k\upsilon - (n+q)\omega_{cs} + p\upsilon}$$

The dielectric tensor for whistler mode wave may be written as $\varepsilon_{11} \pm \varepsilon_{12} = N^2$

Now the dispersion relation for whistler wave is obtained from above relation for $n = 1, p = 1$ and $J_p = 1, J_q = 1$

$$\frac{k^2c^2}{\omega^2} = 1 + \frac{\omega_p^2}{\omega^2}\left[\left(1 + \frac{X_{ac}}{\alpha_\perp}\right)\left\{\frac{\omega}{Mk_\parallel\,\alpha_\parallel} Z(\xi(+ A_T\left(1 + \xi Z(\xi)\right)\right\} + \tan^2\theta_c\left\{\left(\frac{1}{2}\right) + \xi^2\left(1 + \xi Z(\xi) + \frac{X_{ac}}{\alpha_\perp}\xi\left(1 + \xi Z(\xi)\right)\right)\right\}\right]$$

where

$$X_{ac} = \frac{\upsilon\Gamma_x}{\omega_c^2 - \upsilon^2} \qquad X_3 = \frac{\omega_r}{\omega_c} \qquad X_4 = \frac{-\upsilon}{\omega_c} \qquad k_3 = 1 - X_3 + X_4 \;,\; k_4 = \frac{X_3}{k_3}$$

$$k_1 = k_\parallel$$

The required expression for growth rate and real frequency are obtained as

$$\frac{\gamma}{\omega_c} = \frac{\frac{\sqrt{\lambda}}{Mk_1}\left[\left(1 + \frac{X_{ac}}{\alpha_\perp}\right)\left(A_T - k_4\right) + \left(\frac{\tan\theta_c k_3}{Mk}\right)^2 - \frac{X_{ac}\tan\theta_c{}^2 k_3}{\alpha_\perp Mk_1}\right]k_3^3 \exp\left(-\left(\frac{k_3}{Mk_1}\right)^2\right)}{\left(1 + \frac{X_{ac}}{\alpha_\perp}\right)\left\{1 + X_4\frac{M^2A_T(1+X_4)}{2k_3^2} - \frac{M^2k_1^2}{k_3}\left(A_T - k_4\right)\right\} + \frac{X_{ac}\tan\theta_c{}^2}{2\alpha_\perp}}$$

$$X_3 = \frac{k_1^2}{2\beta}\left[1 + X_4\frac{M^2A_T\beta\left(1 + \frac{X_{ac}}{\alpha_\perp}\right)}{(1+X_4)^2} + \frac{X_{ac}\tan\theta_c{}^2 M}{2\alpha_\perp k_1(1+X_4)}\right]$$

where

$$\beta = \frac{k_\beta T_{ll} n_0 \mu_0}{B_0^2}$$

3. Result and Discussions

Following plasma parameters have been adopted for the calculation of the growth rate for the loss-cone driven whistler instability in magnetosphere. Ambient magnet field B_o=2x10^{-7}T, electron density n_o =5x10^6 m^{-3} and magnitude of AC electric field E_o= 20 mV/m has been considered. Temperature anisotropy A_T is supposed to vary from 0.25 to 0.75 and loss-cone angle θ˚ is to vary from 0˚ to 30˚. Electron energy, K_BT_{ll} is taken to be 5KeV, 7.5KeV and 10KeV. Also AC frequency varies from 2 KHz to 6 KHz.

Figure 1 shows the variation of dimensionless growth rate with respect to $\tilde{k}$ for various values of temperature anisotropy A_T, in the presence of magnitude of AC electric field E_o =20mV/m with a frequency of 2 KHz and loss-cone angle θ=10˚. It is observed that the growth rate increases by increasing the value temperature anisotropy for 0.25< $\tilde{k}$ <0.75. It implies that temperature anisotropy behaves like a free energy source for the propagation and amplification of waves. It is observed that in presence of AC electric field, bandwidth increases more in comparison to the case when AC field is absent, this shows AC field has additive effect. So that minimum of electric field magnitude is enough to trigger the whistler emission and increasing the growth rate, thus increasing the power.

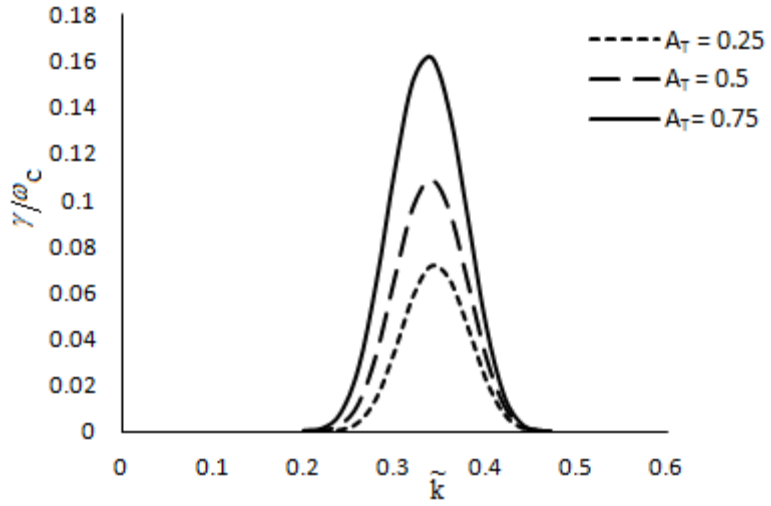

Figure 1: Variation of Growth Rate with respect to $\tilde{k}$ for various values of Temperature Anisotropy at other plasma parameters being B_o= 2x10^{-7}T, E_o= 20mV/m, $K_BT_{||}$= 5KeV, θ = 10˚and υ = 2KHz.

In Figure 2, the variation of dimensionless growth rate with respect to $\tilde{k}$ for different values of loss cone angle θ, in presence of temperature anisotropy has been shown other parameters being listed in figure caption. The graph shows that growth rate increases with increasing the value of loss cone angle and shifting the bandwidth for higher order of loss cone angle. It means that the loss cone angle is also a free energy source to produce the instabilities and propagation of waves.

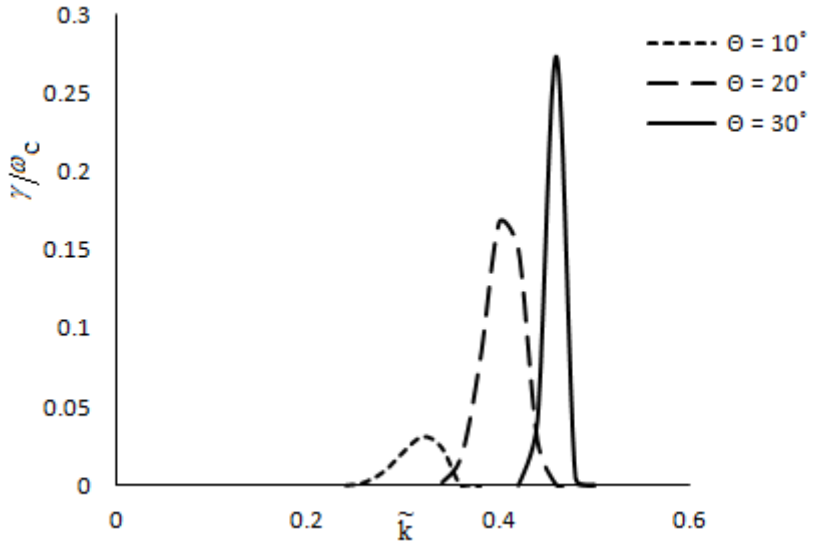

Figure 2: Variation of Growth Rate with respect to $\tilde{k}$ for various values of Loss-cone Angle at other plasma parameters being B_o = 2x10^{-7}T, E_o = 20mV/m, $K_BT_{||}$ = 5KeV, υ = 2KHz and A_T = 0.25

Figure 3 shows the variation of dimensionless growth rate versus $\tilde{k}$ for various values of AC frequency υ , in the case when temperature anisotropy is 0.25, loss-cone angle 10˚ and other parameters being listed in figure caption. The growth rate increases by increasing the AC frequency and the bandwidth is fixed. It represents the modified real frequency of waves.

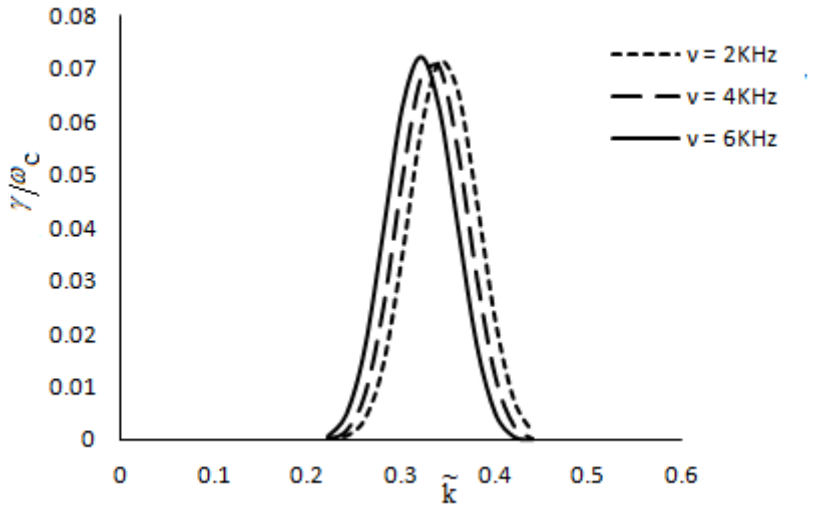

Figure 3: Variation of Growth Rate with respect to $\tilde{k}$ for various values of magnitude of AC Field Frequency at other plasma parameters being $B_o = 2x10^{-7}T$, $E_o = 20mV/m$, $K_BT_{||} = 5KeV$, $\theta = 10^{\circ}$and $A_T = 0.25$

Figure 4 is the graph showing the variation of dimensionless growth rate with respect to $\tilde{k}$ for various values of thermal energy and other parameters being listed in figure caption. The magnitude of electron energy $K_BT_{||}$ has been varied and it is observed that growth rate increases by increasing the thermal energy and the bandwidth increases for the higher order of $\tilde{k}$. This implies emission is possible for extended values of $\tilde{k}$.

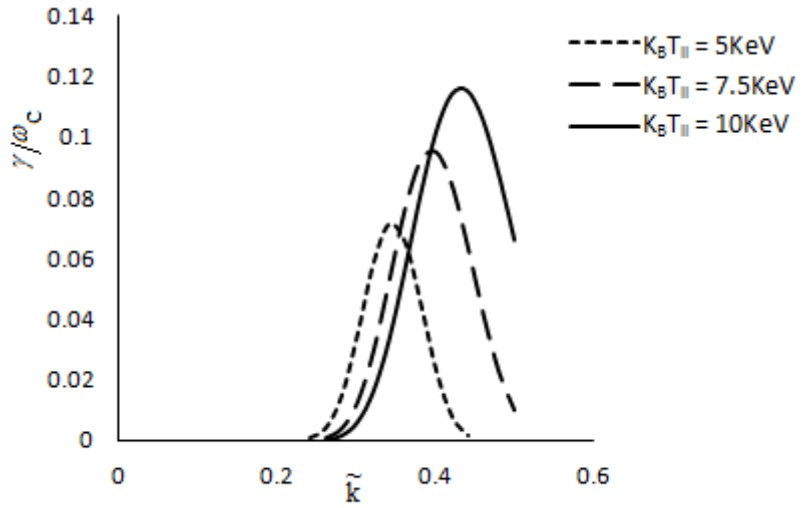

Figure 4: Variation of Growth Rate with respect to $\tilde{k}$ for various values of Electron Energy $K_BT_{||}$ at other plasma parameters being $B_o = 2x10^{-7}T$, $E_o = 20mV/m$, $\theta = 10^{\circ}$, υ = 2KHz and $A_T = 0.25$

In Figure 5 the variation of dimensionless growth rate versus $\tilde{k}$ for various values of loss cone angle for isotropic temperature has been shown and other parameters being listed in figure caption. The growth rate increases and bandwidth shifts for higher value of $\tilde{k}$. It is observed that increase in the growth rate is less for the case of temperature anisotropy. It is clear from figure that even if temperature anisotropy is equal to 0, there is a growth rate. So the instability has been generated due to loss cone angle.

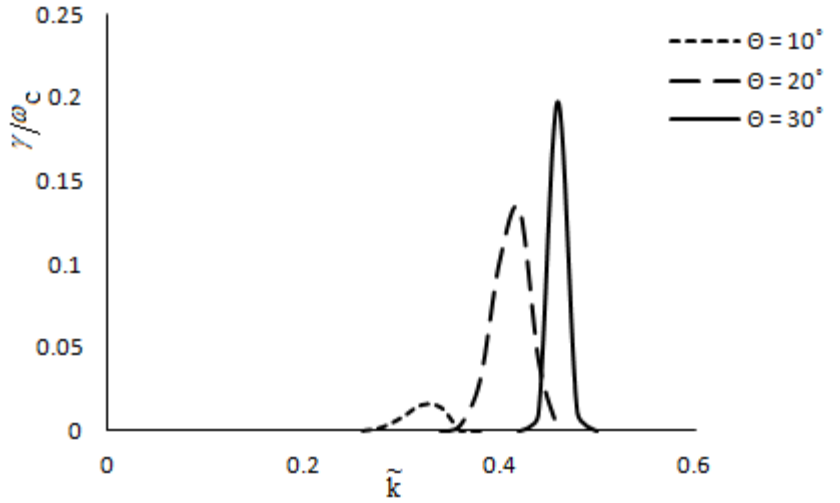

Figure 5: Variation of Growth Rate with respect to $\tilde{k}$ for various values of Loss-cone angle at $A_T = 0$ and other plasma parameters being $B_o = 2x10^{-7}T$, $E_o = 20mV/m$, $K_BT_{\|} = 5KeV$, $\upsilon = 2KHz$.

Figure 6 shows the variation of dimensionless growth rate versus $\tilde{k}$ for various temperature anisotropy for zero loss cone angle and other parameters being listed in figure caption. The graph shows that growth rate increases by increasing the anisotropy for a fixed bandwidth. The increase in the growth rate is less than that in case of non-zero loss cone angle, shown in Figure 1.

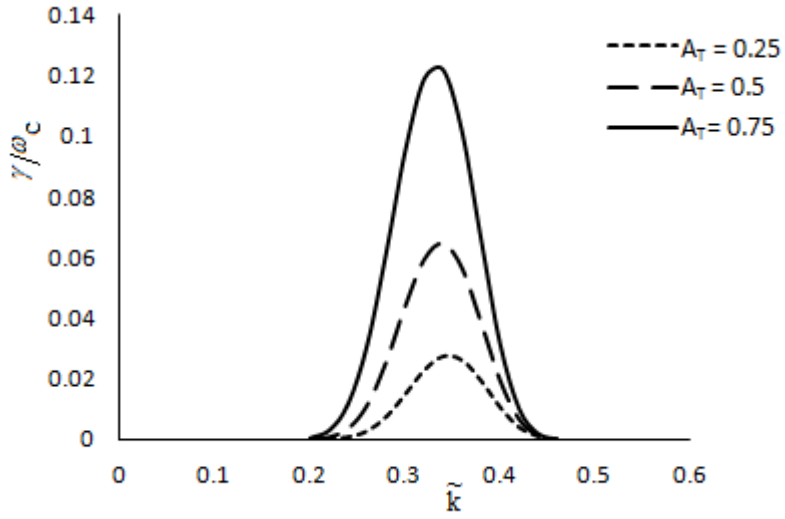

Figure 6: Variation of Growth Rate with respect to $\tilde{k}$ for various values of Temperature Anisotropy at Loss-cone angle $\theta = 0^o$ and other plasma parameters being $B_o = 2x10^{-7}T$, $E_o = 20mV/m$, $K_BT_{\|} = 5KeV$, and $\upsilon = 2KHz$

Conclusion

A comprehensive study of whistler mode emissions using loss cone distribution function in the presence of perpendicular AC electric field has been done. By considering the kinetic approach and applying the method of characteristic solution, numerical calculations have been performed. The derived expressions of dispersion relation and growth rate are analyzed for whistler waves propagating parallel along the ambient magnetic field. The detailed study shows that the growth rate of electromagnetic whistler mode wave increases with increasing temperature anisotropy and loss cone angle. It is also concluded that even in the absence of temperature anisotropy, there is growth of whistler waves. This shows that loss-cone angle is an important free energy source in generating whistler mode instability. Also frequency of AC electric field modifies the resonant frequency conditions of Doppler shift and show the triggering effect.

References

1. R.A. Helliwell, A Theory of Discrete VLF Emissions from the Magnetosphere, Journal of Geophysical Research 72, 4773 (1967).
2. C.F. Kennel and H.E. Petscheck, Limit on stably trapped particle fluxes, Journal of Geophysical Research 71, 128 (1966).
3. U.S. Inan, T.F Bell and R.A. Helliwell, Nonlinear pitch angle scattering of energetic electrons by coherent VLF waves in magnetosphere, Journal of Geophysical Research 83, 3235 (1978).
4. L. Huang, J.G. Hawkins and L.C. Lee, On the Generation of the Pulsating Aurora by the Loss Cone Driven Whistler Instability in the Equatorial Region, Journal of Geophysical Research, 95, 3893 (1990).
5. F. Xiao, Q. Zhou, Huiyoung He and Lijun Tang, Instability of whistler-mode waves by a relativistic kappa-loss-cone distribution in space plasmas, Plasma Physics and Controlled Fusion 48, 1437 (2006).
6. P.R. Prince and G. Renuka, Whistler wave instability and plasma sheet ALC Distribution at substorm onset, Indian Journal of Radio & Space Physics 36, 318 (2007).
7. R.S. Pandey, H. Singh, J. Kishor, N.K Pandey and S. Md. Karim, Pramod Kumar, Generation of obliquely propagating whistler mode instability for inhomogeneous inospheric plasma, Archives of Physics Research 2(3), 1 (2011).
8. R.S. Pandey, U.C Srivastava, A.K Srivastava, S. Kumar and D.K Singh, Pitch Angle Loss-Cone Anisotropic Magneto plasma In Presence of Parallel Electric A.C. Field. Archives of Physics Research 1(4), 126 (2010).